

## Sensitivity Analysis of Ride Behaviour of Indian Railway Rajdhani Coach using Lagrangian Dynamics

**Rakesh Chandmal Sharma**

*Maharishi Markandeshwar University,  
 Mullana, Ambala, India.  
 Email: er\_rcs2000@yahoo.co.in*

### ABSTRACT:

*In this paper, the ride analysis of Rajdhani coach is undertaken using 37 degrees of freedom vertical-lateral coupled vehicle-track model that is formulated using Lagrangian dynamics. The vehicle is considered to be moving along a straight track at a constant speed of 130 kmph. The simulated results of ride behaviour are compared with the experimental data. A sensitivity analysis is carried out in order to investigate the influence of mass and moment of inertia of car body, suspension stiffness, damping coefficient and wheel base on the ride behaviour.*

### KEYWORDS:

*Ride behaviour; Sensitivity analysis; Rail vehicle; Lagrangian dynamics; Vertical ride; Lateral ride*

### CITATION:

R.C. Sharma. 2013. Sensitivity Analysis of Ride Behaviour of Indian Railway Rajdhani Coach using Lagrangian Dynamics, *Int. J. Vehicle Structures & Systems*, 5(3-4), 84-89. doi:10.4273/ijvss.5.3-4.02.

### NOMENCLATURE:

$m_{C,B}$	Mass of car body and bolster respectively.	$t_B$	Lateral distance from bolster c.g. to vertical suspension between bolster and bogie frame.
$m_{BF,W}$	Mass of bogie frame and wheel axle respectively.	$z_{12}$	Vertical distance between the c.g. of car body and bolster.
$I_C^{x,y,z}$	Roll, pitch and yaw mass moment of inertia of car body respectively.	$z_{24}$	Vertical distance between the c.g. of bolster and bogie frame.
$I_B^{x,y,z}$	Roll, pitch and yaw mass moment of inertia of bolster respectively.	$z_{46}$	Vertical distance between the c.g. of bogie frame and its wheel axle.
$I_{BF}^{x,y,z}$	Roll, pitch and yaw mass moment of inertia of bogie frame respectively.	$x_{12}$	Horizontal distance between c.g. of car body and bolster.
$I_W^{x,y,z}$	Roll, pitch and yaw mass moment of inertia of wheel axle respectively.	$x_{46}$	Horizontal distance between the bogie frame c.g. and the corresponding wheel axle c.g.
$k_{CB}^{z,y}$	Vertical (1/2 part) and lateral (1/2 part) stiffness between car body and bolster respectively.	$l_A$	Longitudinal distance from wheel axle c.g. to vertical suspension between bogie frame and wheel axle set.
$c_{CB}^{z,y}$	Vertical (1/2 part) and lateral (1/2 part) damping coefficient between car body and bolster respectively.	$a$	Half of wheel gauge.
$k_{BBF}^{z,y}$	Vertical (1/4 part) and lateral (1/2 part) stiffness between bolster and bogie frame respectively.	$\delta$	Conicity.
$c_{BBF}^{z,y}$	Vertical and lateral damping coefficient between bolster and bogie frame respectively (1/2 part).	$f_{11}$	Lateral creep coefficient
$k_{BFWA}^{z,y}$	Vertical (1/4 part) and lateral (1/2 part) stiffness between bogie frame and wheel axle.	$f_{12}$	Lateral/spin creep coefficient
$c_{BFWA}^{z,y}$	Vertical (1/4 part) and lateral (1/2 part) damping coefficient between bogie frame and wheel axle.	$f_{22}$	Spin creep coefficient
$t_W$	Lateral distance from bogie frame c.g. to vertical suspension between bogie frame and wheel axle.	$f_{33}$	Longitudinal creep coefficient
$t_C$	Lateral distance from car body c.g. to side bearings.		

## 1. Introduction

A railway vehicle is generally evaluated in terms of ride behaviour, stability and curving ability. Ride behaviour is related to a smooth train ride without annoying thrusts or oscillations, disturbing the passenger in his rest or in his activities during journey. The vehicle ride is evaluated in terms of vertical and lateral ride. Moreover there exists a coupling between the vertical and lateral

motions. The vertical irregularities of the track cause both vertical and lateral vibrations in the rail vehicle. In addition, there exists a coupling between vertical & pitch motion and lateral & roll motion for the different rigid bodies of the railway vehicle. In the evaluation of vehicle vertical and lateral ride, the power spectral density (PSD) of acceleration response of the car body mass centre as a function of frequency is of prime interest. In this study a 37 Degrees of Freedom (DoF) vertical-lateral coupled model of Indian Railway Rajdhani coach is formulated using Lagrangian dynamics for investigating the ride behaviour and its sensitivity analysis. The coupled dynamics of rail vehicle has been earlier studied by Zhai et al [6, 10]. The Lagrangian method is generally used for the analysis of coupled vertical-lateral dynamics of moving vehicle. This method is used earlier for the analysis of four wheel road vehicle [12, 13] and three wheel road vehicle [15].

In the past author has also carried out ride [4], eigenvalue and stability analysis [2] of Indian Railway General Sleeper coach using this method. The objective of present work is to examine the rail vehicle parameters that are critical in the context of vertical and lateral ride behaviour. Suarez et al [1] carried out a sensitivity analysis of inertia properties of railway vehicle and found that mass and pitch moment inertia of the vehicle bodies are the most sensitive parameters. Park et al [5] applied surface response method and neural network method to investigate the sensitivity of suspension characteristics on the dynamic behaviour of Korean high speed train. Zakeri and Xia [7] performed a sensitivity analysis of sub-structure parameters and found that a reduction in sleeper spacing, rail pad stiffness, ballast stiffness and increase in ballast damping reduced the contact forces between wheel-rail, rail-sleeper and in sleeper-ballast.

## 2. Mathematical modeling

The mathematical model of a Rajdhani coach of Indian Railway, as shown in Fig. 1 and Fig. 2, is formulated using Lagrangian dynamics with the following assumptions:

- The railway vehicle is symmetric along longitudinal plane.
- Vehicle is travelling at a constant speed such that the longitudinal DoF is not a rigid body motion.
- All springs and dampers are assumed to be linear.
- Creep forces are linear functions of wheel set displacement. Linear Kalker Theory [11] is used for calculation of creep forces.
- Track is considered to be flexible. Its flexibility is accounted by considering wheel to be in series with sleeper, soil and subsoil.
- Car body is assumed to be rigid.
- The contact between wheel and rail is intact.

The 37 DoF of railway vehicle include the following rigid bodies:

- Car body with 5 DoF as vertical, lateral, roll, pitch and yaw ( $y_i, z_i, \theta_i, \phi_i$  and  $\psi_i$  where  $i = 1$  for car body).

- Front and rear bolster each with 3 DoF each as vertical, lateral and roll ( $y_i, z_i$  and  $\theta_i$  where  $i = 2$  for front and 3 for rear bolster).
- Front and rear bogie frame each with 5 DoF as vertical, lateral, roll, pitch and yaw  $y_i, z_i, \theta_i, \phi_i$  and  $\psi_i$  where  $i = 4$  for front and 5 for rear bogie frame).
- Four wheel axles with 4 DoF as vertical, lateral, roll and yaw ( $y_i, z_i, \theta_i, \psi_i$  where  $i = 6, 7, 8$  and 9 for four wheel axles).

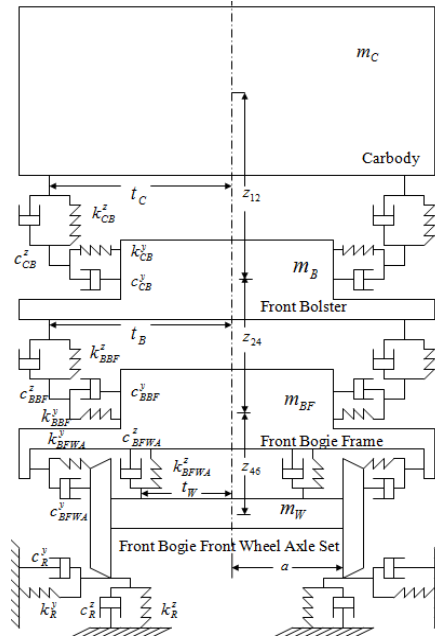


Fig. 1: Rail-vehicle model (side view)

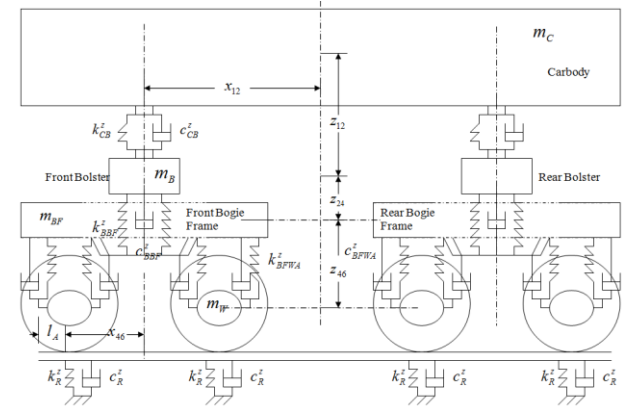


Fig. 2: Rail-vehicle model (front view)

The equations of motion describing coupled vertical-lateral dynamics of the rail-vehicle are obtained using the Lagrangian dynamics as follows,

$$\frac{d}{dt} \left[ \frac{\partial L}{\partial \dot{q}_i} \right] - \frac{\partial L}{\partial q_i} + \frac{\partial E_p}{\partial q_i} + \frac{\partial E_D}{\partial \dot{q}_i} = Q_i \quad (1)$$

Lagrangian operator  $L$  is defined as  $(T - V_g)$ , where  $T$  is the kinetic energy and  $V_g$  is the potential energy due the gravity effect of the vehicle system.  $E_p$  is the energy stored in the system due to springs.  $E_D$  is the Rayleigh's dissipation function of the system.  $Q_i$  are the generalized forces corresponding to the generalized coordinates,  $y_i$ .

The final equations of motion of the rail vehicle are obtained as,

$$[M]\{\ddot{y}_i\} + [C]\{\dot{y}_i\} + [K]\{y_i\} = [F_r(\omega)] \quad (2)$$

Where  $[M]$ ,  $[K]$  and  $[C]$  are the  $37 \times 37$  mass, stiffness and damping matrices respectively for the rail vehicle.  $[F_r(\omega)]$  is a  $37 \times 1$  force matrix for displacement excitations at 8 wheel contact points,  $r = 1, 2, 3, \dots, 8$  due to the vertical and lateral irregularities of the track. Eqn.(2) may further be simplified as,

$$[D_1]H_r(\omega) = F_r(\omega) \quad (3)$$

Where  $[D_1]$  is the dynamic stiffness matrix.  $H_r(\omega) = (y_i/q_r)$  is the complex frequency response function for  $r^{th}$  input. The vertical and lateral irregularities in the railway track surface are random and represented by auto and cross PSD functions as reported by Goel et al [8]. Vertical and lateral irregularities are of the type  $S(\Omega) = C_{sp} \Omega^{-N}$ . Where  $C_{sp}$  is an empirical constant.  $N$  characterizes the rate at which amplitude decreases with frequency. For a linear system subjected to random inputs, the auto and cross PSD matrix of the response is written as,

$$[S_{yy}(\omega)]_{37 \times 37} = [H_r(\omega)]_{37 \times 8} [S_r(\omega)]_{8 \times 8} [H_r(\omega)]_{8 \times 37}^T \quad (4)$$

The complex frequency response functions  $[H_r(\omega)]_{37 \times 8}$  can also be defined as the ratio of response rate to unit harmonic input at a given point. The superscript T denotes transpose of matrix. In the evaluation of vehicle ride quality, the mean square acceleration response (MSAR) as,

$$MSAR = (2\pi f)^4 [H_r(\omega)]_{37 \times 8} [S_r(\omega)]_{8 \times 8} [H_r(\omega)]_{8 \times 37}^T \quad (5)$$

The spectral density of output corresponding to each DOF of car body can be plotted against frequency. To determine the root mean square acceleration response (RMSAR) at a center frequency  $f_c$ , the PSD function is integrated over one third octave band as,

$$RMSAR = \sqrt{[2\pi f]^4 \int_{0.89 f_c}^{1.12 f_c} [S_{yy}(f)](f)^4 df} \quad (6)$$

### 3. Ride analysis

The results from testing are obtained from Research Design Standards Organisation, Lucknow. The rail vehicle is accelerated at a constant speed of 130 kmph over straight track. The data acquisition is completed in two stages. In the first stage the record is obtained for 2 km straight specimen run-down track. This record is verified covering a long run of about 25 km in the second stage. A MEMS based accelerometer is placed at floor level near bogie pivot of the rail vehicle. The acceleration data is recorded in time domain with National Instruments cards (Sampling rate: 100 Samples/s, Resolution: 12 Bit) using LabView. This record is converted in frequency domain using Fast Fourier Transformations. PSD of accelerations in vertical and lateral directions of loaded car body obtained through testing are shown in Fig. 3 and Fig. 4 respectively. The same data obtained through simulation are shown in Fig. 5 and Fig. 6 respectively. The simulation and testing results compare reasonably well except the frequency at peak values.

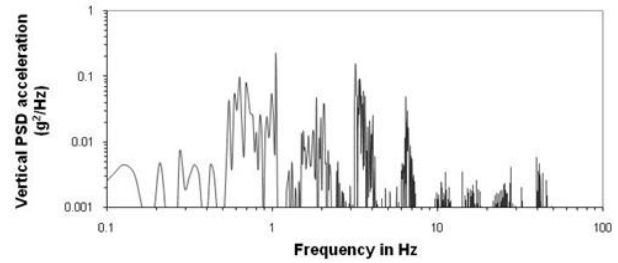


Fig. 3: Vertical acceleration PSD of loaded coach from testing

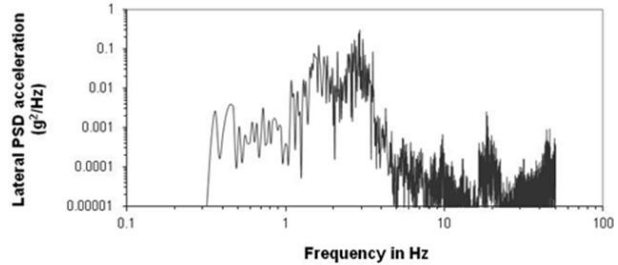


Fig. 4: Lateral acceleration PSD of loaded coach from testing

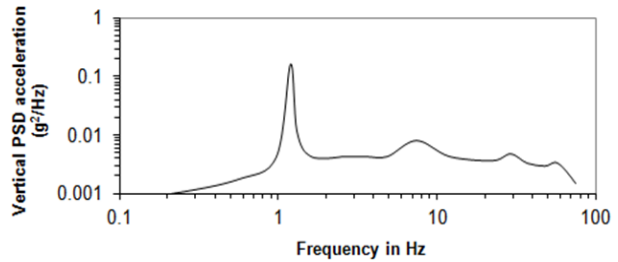


Fig. 5: Vertical acceleration PSD of loaded coach from simulation

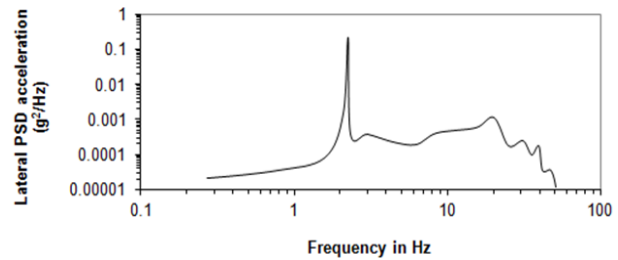


Fig. 6: Lateral acceleration PSD of loaded coach from simulation

The vertical and lateral RMS acceleration values of loaded Rajdhani coach obtained through simulation are shown in Fig. 7 and Fig. 8 respectively. When vertical and lateral ride is judged on the basis of ISO-2631 [17] for 8 hrs comfort criterion, it is found that the vertical ride of loaded Rajdhani coach is uncomfortable in the frequency range of around 1.1 Hz and between 5 and 10 Hz. The lateral ride is uncomfortable around 2.5 Hz.

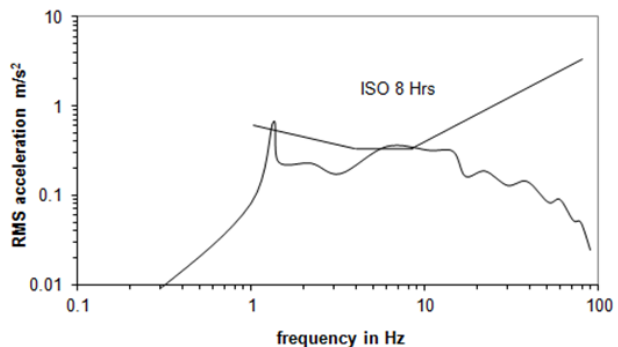


Fig. 7: Vertical RMS acceleration of loaded coach from simulation

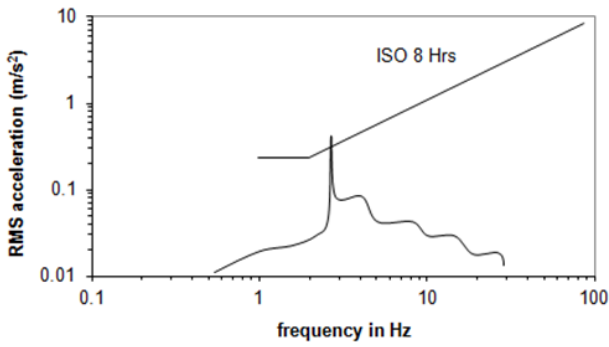


Fig. 8: Lateral RMS acceleration of loaded coach from simulation

#### 4. Sensitivity analysis

Parametric analysis provides the rail vehicle designer with vital information regarding the extent to which each parameter influences the PSD or RMS acceleration response of the vehicle that is moving at a constant speed. This information can be utilized to reach a suitable combination of design parameters to keep the peak value of accelerations within the ISO comfort

boundaries for improved ride behaviour. The ride behaviour of the vehicle is studied by varying one parameter at a time to estimate its individual effect. The parameters taken into consideration are car body mass & its roll, pitch, yaw mass moment of inertia values, spring stiffness & damping coefficient of primary & secondary suspension parameters and wheelbase of bogie frame. The effect of each parameter on the ride behaviour is studied by varying its original value from -20% to +20%. The sensitivity analysis is carried out for the frequencies from 1.1 to 15 Hz as higher frequencies do not affect the human vibration. Lower frequencies are important when motion sickness in passengers has to be evaluated. The values of existing parameters of a loaded Rajdhani coach of Indian Railway listed from Table 1. The values of creep coefficients for the wheel-track interaction have been taken from Yuping & McPhee [9]. The vertical PSD acceleration and lateral values for existing parameter values for Rajdhani coach are mentioned in Table 2 at certain frequencies within the frequency range of human comfort.

Table 1: Rail vehicle parameters of loaded Rajdhani coach

Parameter	Parameter value	Parameter	Parameter value	Parameter	Parameter value	Parameter	Parameter value
$m_C$	33740 kg	$I_{BF}^y$	3206 kg m <sup>2</sup>	$c_{BBF}^z$	0.0589 MN-sec/m	$Z_{46}$	0.209 m
$m_B$	400 kg	$I_{BF}^z$	4763 kg m <sup>2</sup>	$c_{BBF}^y$	1 MN-sec/m	$x_{12}$	7.3915
$m_{BF}$	2600 kg	$I_W^x$	1271 kg m <sup>2</sup>	$k_{BFWA}^z$	0.26454 MN/m	$x_{46}$	1.448 m
$m_W$	1600 kg	$I_W^y$	117 kg m <sup>2</sup>	$k_{BFWA}^y$	11.5 MN/m	$l_A$	0.285 m
$I_C^x$	56932 kg m <sup>2</sup>	$I_W^z$	1271 kg m <sup>2</sup>	$c_{BFWA}^z$	0.0206 MN-sec/m	$a$	0.871 m
$I_C^y$	1307220 kg m <sup>2</sup>	$k_{CB}^z$	35 MN/m	$c_{BFWA}^y$	0.5 MN-sec/m	$\delta$	0.15 rad
$I_C^z$	1309744 kg m <sup>2</sup>	$k_{CB}^y$	17.5 MN/m	$t_C$	0.8 m	$f_{11}$	$7.5848 \times 10^6$ N
$I_B^x$	307 kg m <sup>2</sup>	$c_{CB}^z$	0.0311 MN-sec/m	$t_B$	1.127 m	$f_{12}$	$1.5334 \times 10^4$ N
$I_B^y$	00	$c_{CB}^y$	0.0156 MN-sec/m	$t_W$	1.079 m	$f_{22}$	61.56 N. m <sup>2</sup>
$I_B^z$	336.4 kg m <sup>2</sup>	$k_{BBF}^z$	0.4571 MN/m	$Z_{12}$	1.286 m	$f_{33}$	$8.6605 \times 10^6$ N
$I_{BF}^x$	1713 kg m <sup>2</sup>	$k_{BBF}^y$	0.2066 MN/m	$Z_{24}$	0.1435 m	---	-----

Table 2: Vertical and lateral PSD acceleration values relevant to human vibration

Vertical ride		Lateral ride	
Frequency (Hz)	Acceleration PSD (m/s <sup>2</sup> ) <sup>2</sup> /Hz	Frequency (Hz)	Acceleration PSD (m/s <sup>2</sup> ) <sup>2</sup> /Hz
1.1	20.2	2.5	19.2
3	0.384	4	0.03
5	0.48	7	0.035
8	0.44	10	0.05
10	0.39	15	0.09

The mass, roll, pitch and yaw mass moment of inertia of car body parameters are varied in the analysis.

It has been observed that the car body mass affects both vertical and lateral PSD acceleration responses. Higher value of car body mass than the existing values is preferred for vertical and lateral acceleration PSD in critical frequency region as observed in Fig. 9 and Fig. 10. The pitch mass moment of inertia has no effect on lateral PSD acceleration. Increased pitch mass moment of inertia from existing values is desirable for vertical PSD acceleration in low and high frequency region. The roll mass moment of inertia has negligible effect on vertical PSD acceleration, and marginally it influences the lateral PSD acceleration at critical frequency. The yaw mass moment of inertia has no effect on vertical PSD acceleration.



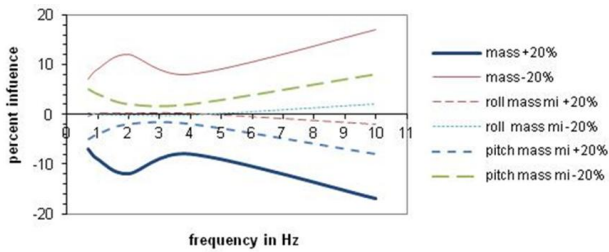


**Fig. 9:** Sensitivity of car body mass and mass moment of inertia on vertical ride

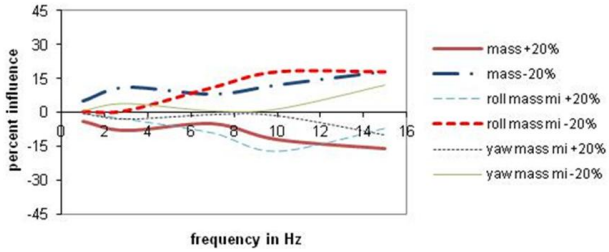


**Fig. 10:** Sensitivity of car body mass and mass moment of inertia on lateral ride

Reducing the secondary suspension vertical stiffness value from the existing value is preferred for vertical PSD acceleration as the acceleration values in all frequency region of human interest is reduced as observed in Fig. 11. Reducing the secondary suspension vertical stiffness value is preferred for lateral PSD acceleration as the peak acceleration value is slightly reduced at critical frequency as observed in Fig. 12. Reducing the secondary suspension vertical damping coefficient value from the existing value is preferred for vertical PSD acceleration as the acceleration is significantly reduced in frequency regions of human interest. Secondary suspension vertical damping has negligible effect on lateral PSD acceleration. Reducing the secondary suspension lateral stiffness and increasing the secondary suspension lateral damping coefficient values from the existing values can be preferred for lateral PSD acceleration as the acceleration values are significantly reduced in all critical frequency regions.

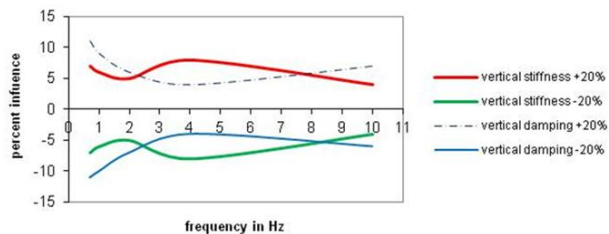


**Fig. 11:** Sensitivity of secondary suspension stiffness on vertical ride

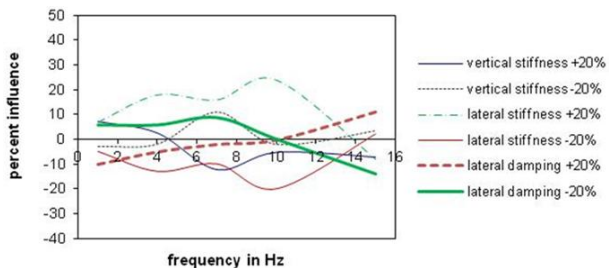


**Fig. 12:** Sensitivity of secondary suspension parameters on lateral ride

Reducing the primary suspension vertical stiffness value from the existing value is preferred for the vertical PSD acceleration as the acceleration values are significantly reduced in the middle and higher frequency region with slight penalty in lower frequency region before 1.8 Hz as observed in Fig. 13. However lateral PSD acceleration is increased slightly at critical frequency with reduction in primary suspension vertical stiffness from existing value as observed in Fig. 14. The vertical PSD acceleration values in all frequency regions are reduced with reduction in primary suspension vertical damping coefficient value from the existing value. Increasing the primary suspension lateral stiffness and damping values from the existing values are preferred for lateral PSD acceleration as the acceleration values are significantly reduced in almost all frequency regions as observed in Fig. 14. Primary suspension lateral stiffness and lateral damping have negligible effect on the vertical PSD acceleration.

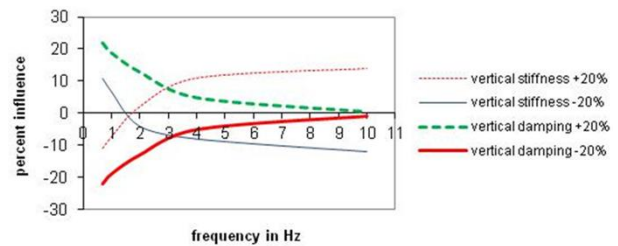


**Fig. 13:** Sensitivity of primary suspension parameters on vertical ride

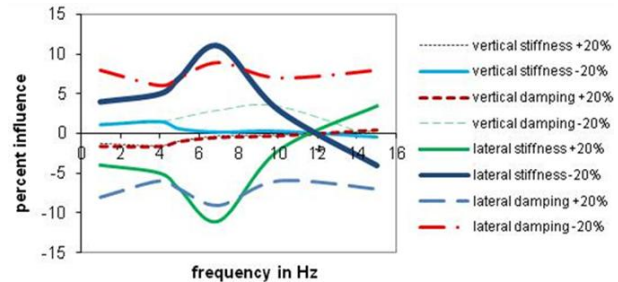


**Fig. 14:** Sensitivity of primary suspension parameters on lateral ride

Reducing the wheelbase from the existing value reduces the vertical PSD acceleration in lower and middle frequency regions (from 1 to 4 Hz) and increases the vertical PSD acceleration in high frequency regions (from 4 to 10 Hz) observed in Fig. 15. Significant reduction in lateral acceleration is observed at critical frequency for reduced wheelbase of bogie frame from the existing value as observed in Fig. 16.

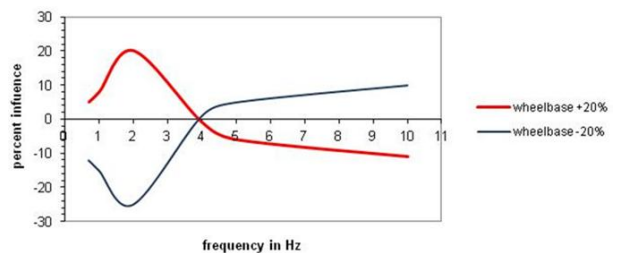


**Fig. 15:** Sensitivity of wheelbase on vertical ride

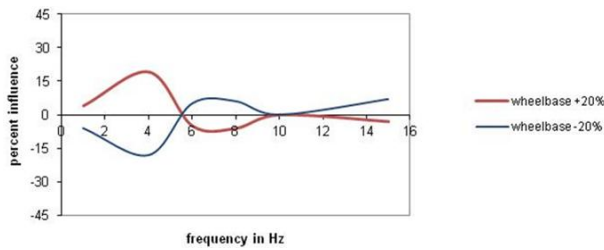


Fig. 16: Sensitivity of wheelbase on lateral ride

## 5. Concluding remarks

The rail-vehicle model of Indian Railways Rajdhani coach was developed using Lagrangian dynamics. Ride behaviour of loaded coach was simulated and the PSD of vertical and lateral accelerations were compared with test results. The simulation results were found to be in good agreement with test. A sensitivity analysis of ride behaviour for  $\pm 20\%$  variation in the existing vehicle parameters was undertaken to improve the comfort in vehicle ride on track with track irregularities. In order to improve the vertical and lateral PSD acceleration, the car body mass and inertia have to be increased. From existing values .Reducing in the primary & secondary suspension and wheel base were also improved the ride behaviour. Further investigations may be focussed on addressing the impact of these variations in vehicle parameters on the track wear and vehicle stability on curved tracks.

## REFERENCES:

- [1] B. Suarez, J. Felez, J. Maroto and P. Rodriguez. 2013. Sensitivity analysis to assess the influence of the inertial properties of railway vehicle bodies on the vehicle's dynamic behaviour, *Vehicle System Dynamics*, 51(2), 2013. <http://dx.doi.org/10.1080/00423114.2012.725851>.
- [2] R.C. Sharma. 2013. Stability and eigenvalue analysis of an Indian railway general sleeper coach using Lagrangian dynamics, *Int. J. Vehicle Structures & Systems*, 5(1), 9-14. <http://dx.doi.org/10.4273/ijvss.5.1.02>.
- [3] R.C. Sharma. 2012. Recent advances in railway vehicle dynamics, *Int. J. Vehicle Structures & Systems*, 4(2), 52-63. <http://dx.doi.org/10.4273/ijvss.4.2.04>.
- [4] R.C. Sharma. 2011. Ride analysis of an Indian railway coach using Lagrangian dynamics, *Int. J. Vehicle Structures & Systems*, 3(4), 219-224. <http://dx.doi.org/10.4273/ijvss.3.4.02>.
- [5] C. Park, Y. Kim and D. Bae. 2009. Sensitivity analysis of suspension characteristics for Korean high speed train, *J. Mechanical Sci. and Tech.*, 23, 938-941. <http://dx.doi.org/10.1007/s12206-009-0316-5>.
- [6] W.M. Zhai, K. Wang and C. Cai. 2009. Fundamentals of vehicle-track coupled dynamics, *Vehicle System Dynamics*, 47(11), 1349-1376. <http://dx.doi.org/10.1080/00423110802621561>.
- [7] J.A. Zakeri and H. Xia. 2008. Sensitivity analysis of track parameters on train-track dynamic interaction, *J. Mechanical Sci. and Tech.*, 22, 1299-1304. <http://dx.doi.org/10.1007/s12206-008-0316-x>.
- [8] V.K. Goel, M. Thakur, K. Deep and B. p. Awasthi. 2005. Mathematical model to represent the track geometry variation using PSD, *Indian Railway Technical Bulletin*, LXI(312-313), 1-10.
- [9] H. Yuping and J. McPhee. 2002. Optimization of the lateral stability of rail vehicles, *Vehicle System Dynamics*, 38(5), 36-90. <http://dx.doi.org/10.1076/vesd.38.5.361.8278>.
- [10] W.M. Zhai, C.B. Cai and S.Z. Guo. 1996. Coupling Model of vertical and lateral vehicle/track interactions, *Vehicle System Dynamics*, 26(1), 61-79. <http://dx.doi.org/10.1080/00423119608969302>.
- [11] J.J. Kalker. 1979. Survey of wheel-rail contact theory, *Vehicle System Dynamics*, 8, 317-358. <http://dx.doi.org/10.1080/00423117908968610>.
- [12] N.S. Nathoo and A.J. Healey. 1978. Coupled vertical-lateral dynamics of a pneumatic tired vehicle: Part 1- A mathematical model, *J. Dynamic System Measurement and Control*, 100,311-318.<http://dx.doi.org/10.1115/1.3426383>.
- [13] N.S. Nathoo and A.J. Healey. 1978. Coupled vertical-lateral dynamics of a pneumatic tired vehicle: Part 2- Simulated versus experimental data, *J. Dynamic System Measurement and Control*, 100,319-325. <http://dx.doi.org/10.1115/1.3426384>.
- [14] A. Watari and S. Iwamoto. 1974, Application of sensitivity analysis to vehicle dynamics, *Vehicle System Dynamics*, 3, 1-16. <http://dx.doi.org/10.1080/00423117408968444>
- [15] K. Ramji. 2004. *Coupled Vertical-Lateral Dynamics of Three-Wheeled Motor Vehicles*, PhD. Dissertation, Dept of Mech. and Industrial Engg., IIT Roorkee, India.
- [16] A.H. Wickens. 2003. *Fundamentals of Rail Vehicle Dynamics*, Swets & Zeitlinger Publishers, Netherlands. <http://dx.doi.org/10.1201/9780203970997>.
- [17] ISO 2631. 1997. *Mechanical Vibration and Shock Evaluation of Human Exposure to Whole Body Vibrations- Part 1: General Requirements*.